

Hydrodynamic Parameters of Pulse Tube or Stirling Cryocooler Regenerators for Periodic Flow

J.S. Cha, S.M. Ghiaasiaan, J.P. Harvey², P.V. Desai,
and C.S. Kirkconnell²

G.W. Woodruff School of Mechanical Engineering
Georgia Institute of Technology,
Atlanta, GA 30332-0405, U.S.A

²Raytheon Space and Airborne Systems (RSAS)
El Segundo, CA 90245-0902, U.S.A.

ABSTRACT

Recent studies have shown that computational fluid dynamics (CFD) techniques can be applied for modeling cryocooler systems in their entirety in order to capture their operation under steady periodic flow. However, the results of CFD simulations can only be fully trusted if they are based on correct closure relations. Among the most important closure relations are the hydrodynamic and heat transfer parameters. The regenerator is typically a microporous structure that is subject to a periodic flow of a cryogenic fluid (gas). The hydrodynamic and heat transfer parameters of microporous structures under oscillatory flow are not well understood, however, and current state of art modeling methods are often based upon using experimentally derived empirical relationships (friction factor and Nusselt number) which are all calculated based on the local, instantaneous flow conditions.

The preliminary results of a research program on the measurement and correlation of hydrodynamic parameters of some widely-used cryocooler regenerator fillers under periodic oscillatory flow conditions are presented. An experimental apparatus consisting of test sections for the measurement of lateral (radial) permeability and Forchheimer coefficients is used. The test section for the radial hydrodynamic parameter measurements is annular. It is connected to a compressor through its inner boundary and to a constant-volume chamber through its outer boundary. The instrumentation includes a function generator, data acquisition system, and pressure transducers. Time histories of local static pressures at points near the entrance and exit of the porous structure are measured under steady-periodic conditions. A CFD-assisted methodology is then applied for the analysis and interpretation of the measured data. The permeability and Forchheimer parameter values obtained in this way are then correlated in terms of relevant dimensionless parameters.

INTRODUCTION

The crucial role of a regenerator in various Pulse Tube Refrigerator (PTR) designs is well recognized. Typically, a PTR regenerator is a complex porous structure that interacts hydrodynamically

cally and thermally with a periodic flow of the working fluid. Ideal regenerator characteristics would include infinite thermal inertia per unit volume, infinite volumetric heat transfer coefficients with the working fluid, and no pressure drops, constant gas properties, and negligible dispersion. In reality, such regenerators are unavailable, and a compromise between pressure drop and heat transfer is required for system level optimization. Recent investigations have shown that current computational fluid dynamic (CFD) tools are in fact capable of simulating entire PTR devices [1-4], and can be useful tools for the final stages of design and optimization. These simulations provide detailed system and component-level information about the flow field and heat transfer processes that are beyond the current experimental measurement possibilities. However, such detailed design and optimization calculations are only reliable if the properties of all the components, in particular the regenerator, are known with reasonable accuracy. The existing regenerators are generally composed of micro porous solid structures, most of which are morphologically anisotropic. The hydrodynamic and thermal transport properties of the most widely-used regenerator filler materials are not well-understood, however. Among the poorly-understood and badly-needed properties are the permeability and inertia coefficient matrices, as well as the solid-fluid volumetric heat transfer coefficients under steady and periodic flow conditions.

Our recent CFD-based investigations on PTRs have shown that significant multidimensional flow effects may occur at the vicinity of component-to-component junctions. Secondary-flow recirculation patterns can develop when one or more components of the PTR system have small length-to-diameter (L/D) ratios, particularly in the presence of large area step changes between components [3, 4]. Among the components of the Inertance Tube PTR (ITPTR) systems that were simulated, the regenerator and pulse tube showed the strongest multidimensional flow effects [4]. The occurrence of multidimensional flow effects further confirms the need for the lateral (radial) hydrodynamic properties of the regenerator. However, previously published experimental studies dealing with materials that are used as regenerator fillers have dealt with friction factors in the axial direction only [5-8]. Recently, we have experimentally measured the radial pressure drop and correlated friction factor for stainless steel 325 mesh screens [9]. However, the latter correlation was derived based on steady flow analysis.

In this paper, we report on periodic flow experiments aimed at the measurement of lateral (radial) permeability and coefficient of inertia (Forchheimer's coefficient) for stainless steel 400 mesh sintered regenerator fillers with 63.2 % porosity.

TEST APPARATUS

The test apparatus is schematically displayed in Figs. 1 and 2, and includes a function generator, a data acquisition system, an amplifier, a compressor, two PCB piezo pressure transducers, and a specially designed annular test section with a chamber enclosure that contains the sintered regenerator. The entire test section contains research grade helium with a nominal purity of 99.9999%. A 4.29 cubic centimeter (cc) swept volume Hughes Tactical Condor compressor is used to stimulate oscillatory flow in the entire test section.

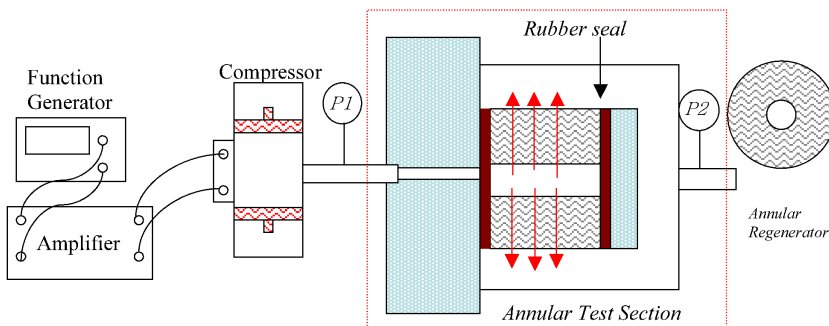


Figure 1. Radial Oscillatory Pressure Drop Test Apparatus.

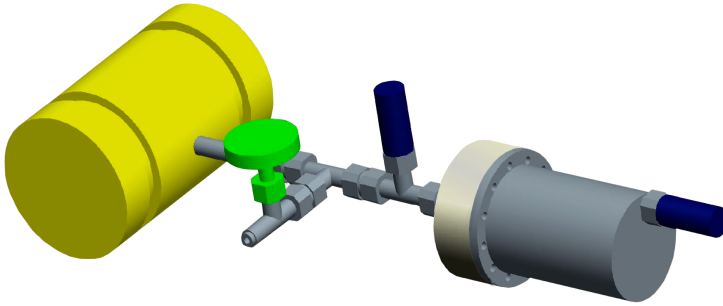


Figure 2. CAD drawing of the experimental test apparatus.

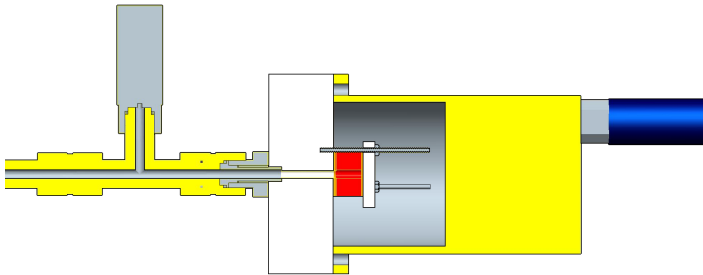


Figure 3. Details of the test section and its vicinity.

Details of the test section are depicted in Figure 3. It consists of a straight 3 mm inner diameter circular tube that leads to a sintered 400 mesh regenerator with inner and outer diameters of 4 mm and 20 mm, respectively. The annular structure was constructed in the following manner. Three stainless steel rods were first threaded perpendicularly onto an aluminum slab 30 mm long and 90 mm in diameter. A 3 mm-diameter hole was drilled through the aluminum slab, which served as the inlet channel to the annular porous structure. The three rods were equally spaced such that a 20-mm diameter cylinder could be tightly housed between them. Thus, the rods form three rigid supports for the 20 mm-diameter circular sintered regenerator.

The annular-shaped sintered regenerator with inner and outer diameters of 4 mm and 20 mm, respectively, was prepared by diffusion-bonding and Electron Discharge Machining (EDM), and was provided by the Raytheon SAS Company. The sintered 400 mesh regenerator was fitted between the depicted rubber seals. The right-end of the regenerator (the right side, in Figure 3) was sealed off by pressing a circular, 5 mm-thick aluminum plate against the regenerator via tightening the three hexagonal nuts on to the threaded rods. The constructed test section thus formed a leak free system, where gas could only leave through the outer surface of the annular porous structure. Furthermore, a constant volume of 174 cc stainless steel chamber is used to fully enclose the entire porous medium. At the interface between the stainless chamber and the base aluminum, a Viton O-ring seal was used to prevent any leakage in the system.

The two piezo pressure transducers (model A101A05 from PCB Electronics) were used to measured the local instantaneous pressures and have a response time of less than 2 μ sec, a range of 0 to 689 kPa (0-100 psi), a resolution of 0.014 kPa (0.002 psi), and a sensitivity of 7.3 mV/kPa (50mV/psi).

CFD MODEL

FLUENT, a commercially available CFD code, is used to model the entire annular test section, shown in Fig. 3, in order to facilitate the interpretation of the experimental data. Given the configuration of the test section, axi-symmetric, two-dimensional flow was assumed.

The simulated system evidently has two completely different parts. For the open parts, the unsteady mass, momentum and energy equations solved by Fluent [10] are, respectively:

$$\frac{\partial \rho_f}{\partial t} + \frac{1}{r} \frac{\partial}{\partial r} [r \rho_f v_r] + \frac{\partial}{\partial x} [\rho_f v_x] = 0 \quad (1)$$

$$\frac{\partial}{\partial t} [\rho_f \bar{v}] + \nabla \cdot [\rho_f \bar{v} \bar{v}] = -\nabla p + \nabla \cdot \bar{\tau} \quad (2)$$

$$\frac{\partial}{\partial t} [\rho_f E] + \nabla \cdot [\bar{v} (\rho_f E_f + p)] = \nabla \cdot [k_f \nabla T + (\bar{\tau} \cdot \bar{v})] \quad (3)$$

where

$$E = h - \frac{p}{\rho_f} + \frac{v^2}{2} \quad (4)$$

All properties represent the Newtonian working fluid, helium. The above equations apply to all sections except for the annular porous structure (i.e., the stainless steel 400 mesh sintered regenerator). The latter region is modeled as an isotropic porous medium with the assumption of local thermal equilibrium between the porous structure and the working fluid. The single phase volume-averaged unsteady mass, momentum, and energy equations for this region can be represented as

$$\frac{\partial}{\partial t} [\varepsilon \rho_f] + \frac{1}{r} \frac{\partial}{\partial r} [\varepsilon r \rho_f v_r] + \frac{\partial}{\partial x} [\varepsilon \rho_f v_x] = 0 \quad (5)$$

$$\frac{\partial}{\partial t} [\varepsilon \rho_f \bar{v}] + \nabla \cdot [\varepsilon \rho_f \bar{v} \bar{v}] = -\varepsilon \nabla p + \nabla \cdot [\varepsilon \bar{\tau}] - \left[\mu \bar{\beta}^{-1} \cdot \bar{j} + \frac{1}{2} \rho_f \bar{C} \cdot |\bar{j}| \bar{j} \right] \quad (6)$$

$$\frac{\partial}{\partial t} [\varepsilon \rho_f E_f + (1-\varepsilon) \rho_s E_s] + \nabla \cdot [\bar{v} (\rho_f E_f + p)] = \nabla \cdot [\varepsilon k_f + (1-\varepsilon) k_s] \nabla T + (\varepsilon \bar{\tau} \cdot \bar{v}) \quad (7)$$

here $\bar{\beta}$ and \bar{C} represent the permeability and the Forchheimer coefficient tensors. Note that all velocities are volume-averaged intrinsic velocities, which are related to the volume-averaged superficial velocities according to $\bar{j} = \bar{U} \bar{v}$. Since the axial (x) and radial (r) coordinates are the principal directions of the porous medium, the latter matrices are diagonal. The bracketed term on the right side of Eq. (6) will be:

$$\mu \beta_i^{-1} j_i + \frac{1}{2} C \rho_f |\bar{j}| j_i = \frac{1}{2} \frac{f_i}{\sqrt{\beta_i}} \rho_f |\bar{j}| j_i \quad (8)$$

where $i = x$ and r for axial and radial directions, respectively.

Periodic flow CFD simulations for the entire test section depicted in Figure 3 were performed using approximately 7000 mesh nodes. Using the latter mesh size, 100 time steps were needed for a complete cycle. With further reduction of the time step size by a factor of $1/2$, no significant changes were observed in the CFD solutions. The boundary conditions included known inlet instantaneous static pressure as a periodic function of time.

RESULTS OF EXPERIMENTS

A total of seven oscillatory radial pressure drop tests was conducted using the 400 mesh sintered stainless steel regenerator with porosity of 63.2%. Each test represented a fixed compressor frequency, and the seven tests covered the frequency range 5 to 60 Hz. In six of the tests (excluding a test at 5 Hz) the peak-to-peak sinusoidal voltage amplitude was first increased via the function generator, starting from a near-zero value, until either the maximum compressor piston displacement or the maximum current limit was reached. The voltage amplitude was then maintained constant, and the pressures at P1 and P2 were recorded after steady periodic conditions were established. For the 5 Hz frequency, however, low flow conditions were sought so that the permeability in Darcy flow conditions could be tested, therefore the peak-to-peak sinusoidal voltage amplitude was increased only sufficiently to ensure that pressure sensor signals were viable.

Table 1. Experimental measured data.

| Freq (hz) | 5 | 10 | 20 | 30 | 40 | 50 | 60 |
|--------------------|--------|---------|---------|---------|---------|---------|---------|
| P1 | | | | | | | |
| \hat{M}_1 , [Pa] | 2456.1 | 40052.8 | 45161.1 | 50419.8 | 26913.3 | 17133.6 | 11912.1 |
| \hat{M}_2 , [Pa] | 6.3 | 196.4 | 119.0 | 467.2 | 274.5 | 153.5 | 105.7 |
| \hat{M}_3 , [Pa] | 158.3 | 1007.9 | 1385.3 | 3243.1 | 1364.5 | 850.0 | 604.3 |
| ψ_1 , [Deg] | -110.3 | -115.8 | -143.3 | -158.5 | -168.9 | -176.7 | 176.6 |
| ψ_2 , [Deg] | -58.3 | 68.1 | 5.0 | -78.8 | -92.9 | -121.4 | -131.3 |
| ψ_3 , [Deg] | -153.7 | 53.4 | -169.7 | 73.5 | 13.7 | -33.4 | -74.5 |
| P2 | | | | | | | |
| \hat{M}_1 , [Pa] | 2063.8 | 33762.8 | 37150.1 | 38584.1 | 20410.0 | 12834.2 | 8806.7 |
| \hat{M}_2 , [Pa] | 4.1 | 149.0 | 42.0 | 121.4 | 108.1 | 68.7 | 47.3 |
| \hat{M}_3 , [Pa] | 133.7 | 1014.0 | 620.2 | 414.5 | 56.4 | 74.8 | 64.2 |
| ψ_1 , [Deg] | -113.3 | -122.8 | -160.5 | 171.4 | 156.9 | 144.2 | 132.5 |
| ψ_2 , [Deg] | 5.5 | 87.3 | 25.3 | -154.4 | -141.4 | 173.5 | 137.4 |
| ψ_3 , [Deg] | -161.5 | 36.1 | -139.5 | 32.0 | -111.0 | 161.4 | 116.6 |

The recorded pressure data were steady periodic. In order to simplify the analysis, they were first transformed to the frequency domain by Fast Fourier Transforms (FFT), and were thereby represented as Fourier cosine series. It was noticed that the first three harmonics were sufficient for the accurate replication of the actual measured waveforms. The measured steady periodic pressures could thus be represented as:

$$P_i(t) = \hat{M}_1 \cos(\lambda_1 t + \psi_1) + \hat{M}_2 \cos(\lambda_2 t + \psi_2) + \hat{M}_3 \cos(\lambda_3 t + \psi_3) \quad (9)$$

where $i=1$ and 2. Table 1 is a summary of all the parameters in the above equation.

RESULTS AND DISCUSSION

CFD simulations were performed for all the measured data. The objective, as mentioned before, was to obtain the radial permeabilities and coefficients of inertia by trial and error. To do this, the axial permeability and coefficient of inertia were needed, since the simulations were axisymmetric two dimensional. The porous structure was assumed to be isotropic, due to the unavailability of axial flow parameters for the tested 400 mesh sintered regenerator at this time. The error caused by this assumption is likely to be small, however, because the simulation results indicate that axial flows were everywhere negligibly small in comparison with radial flows. A User Defined Function (UDF) for Fluent was developed, whereby, for each frequency, Eq. (9) with parameters representing P1 was applied as the inlet boundary condition in the corresponding CFD simulations. The predicted CFD results for pressure amplitude and phase at P2 could then be directly compared with the experimental data or Eq. (9) with parameters representing P2 for verification. Simulations were iteratively repeated by adjusting the radial hydrodynamic parameters β_r and C_r . Very good agreement between data and simulations results was obtained with $\beta_r = 5.348\text{e-}12 \text{ m}^2$ and $C_r = 240000$.

Figures 4(a), (b), (c), (d), (e), and (f), display comparisons between the experimental pressure drops at location P2 with the simulated pressure drops. These figures show that for frequencies of 30 Hz and higher the experimental data and simulation results are in excellent agreement with respect to the pressure oscillation magnitude and phase. At the lower frequencies, 5 Hz, 10 Hz, and 20 Hz, however, the simulations over predict the phase difference between the pressure waves at

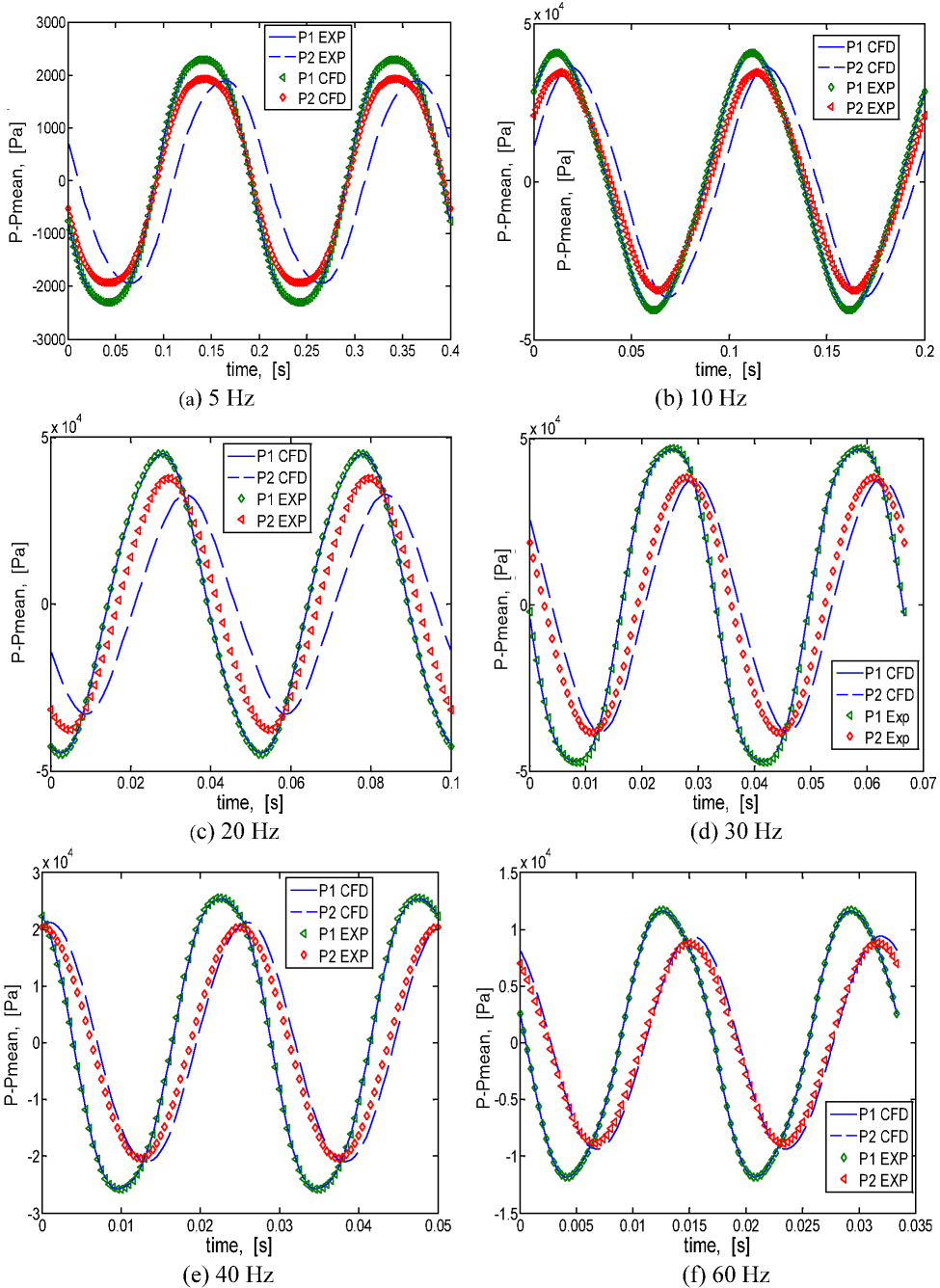


Figure 4. Experimental oscillatory pressure drops and CFD simulation results.

the two locations. Thermo-acoustic resonance in the test apparatus may be a possible explanation for this phase difference. Alternative to the definition of permeability and Forchheimer coefficients is the friction factor, defined in Eq. (8). Based on the our data for the tested stainless steel 400 mesh sintered regenerator with 63.2% porosity, the following correlations could be developed:

$$f = \frac{a}{\text{Re}_r} + b \quad (10)$$

$$\text{Re}_r = \frac{\rho_f v_r \sqrt{\beta_r}}{\mu} \quad (11)$$

In the investigation reported here, the methodology was applied for the quantification of the radial flow parameters for the 400 mesh sintered stainless steel filler with 63.2% porosity. Periodic pressure drops were measured in an apparatus that consisted of an annular porous test section for inlet pressure oscillations with 5 to 60 Hz frequencies. By iterative CFD simulations, the aforementioned hydrodynamic parameters were calculated. The results of these measurements enable more accurate calculation of multidimensional flow effects in small aspect ratio cryocooler components.

ACKNOWLEDGMENT

The authors acknowledge gratefully the financial and technical support for this work by Raytheon SAS Company. The authors also like to thank Ms. Melina Pillar of Raytheon SAS for providing the porous media samples.

NOTATION

a, b = Correlation Coefficients

\overline{C}, C_r = Inertial Drag Coefficient Tensors

f = Friction Factor

h = Enthalpy

j = Superficial Velocity

k = Thermal Conductivity

\hat{M}_i = FFT Pressure Amplitudes, $i = 1, 2, 3$

T = Temperature

v = Intrinsic Velocity

Greek letters

$\overline{\beta} = \beta_r$ = Permeability Tensors

ε = Porosity

$\lambda_i = i\omega, \omega = 2\pi \text{freq}, i=1,2,3$

μ = Absolute viscosity

ρ = Density

$\overline{\tau}$ = Stress tensors

ψ_i = FFT Pressure Phases, $i=1,2,3$

Subscripts

f = Fluid, r = Radial coordinate

s = Solid, x = Axial coordinate

REFERENCES

- Hozumi, Y., Shiraishi, M., and Murakami, M., "Simulation of Thermodynamics Aspects about Pulse Tube Regenerators," *Adv. in Cryogenic Engineering*, Vol. 49, edited J. Waynert et al., pp. 1500-1507.
- Flakes, B., and Razani, A., "Modeling Pulse Tube Cryocoolers with CFD," *Adv. in Cryogenic Engineering* 49, edited J. Waynert et al., pp. 1493-1499.
- Cha, J.S., *CFD Simulation of Multi-dimensional Effects in an Inertance Tube Pulse Tube Refrigeration*, Masters Thesis, Georgia Institute of Technology, Atlanta, Georgia (2004).
- Cha, J.S., Ghiaasiaan, S.M., Desai, P.V., Harvey, J.P., and Kirkconnell, C.S. "CFD Simulation of Multi-dimensional Effects in an Inertance Tube Pulse Tube Refrigeration," *Cryocoolers 13*, Kluwer Academic/Plenum Publishers, New York (2005), pp. 285-292.
- Kays, W. and London, A., *Compact Heat Exchangers*, McGraw-Hill, Inc., NY (1964), pp. 148-149.
- Miyabe, H., Takahashi, S., and Hamaguchi, K., "An approach to the design of Stirling engine regenerator matrix using packs of wire gauzes," *Proc. 17th IECE*, Vol. 1 (1982), pp. 1839-1844.
- Ju, Y., Jiang, Y., and Zhou, Y., "Experimental study of the oscillating flow characteristics for a regenerator in a pulse tube cryocooler," *Cryogenics*, Vol. 38, No. 6 (June 1998), pp. 649-656.
- Harvey, J.P., *Oscillatory compressible flow and heat transfer in porous media – application to cryocooler regenerators*, Ph.D. Thesis, Georgia Institute of Technology, Atlanta, Georgia (2003).
- Cha, J.S., Ghiaasiaan, S.M., and Desai, P.V., "Measurement of Anisotropic Hydrodynamic Parameters of Pulse Tube or Stirling Cryocooler Regenerators," *Adv. in Cryogenic Engineering*, Vol. 51, Amer. Institute of Physics, Melville, NY (2006), pp.1911-1918.
- Fluent INC., *Fluent 6 User Manual* (2003), p. 8-1.